
A 3-Dimensional Atmospheric Neutrino Flux Calculation

G. Barr¹, T.K. Gaisser², Paolo Lipari³, S. Robbins¹, & Todor Stanev²

(1) *Dept. of Physics, Oxford University, UK*

(2) *Bartol Research Institute, University of Delaware, Newark, DE, USA*

(3) *INFN, Università di Roma (La Sapienza), ITALY*

Abstract

A full 3-dimensional code has been developed within the framework of the Bartol atmospheric neutrino flux calculations [1,2], which until now have been made in the one-dimensional approximation. Bending of primaries and secondaries within a realistic geomagnetic field is included. The ultimate goal is to provide a new set of neutrino fluxes for use in interpretation of measurements of atmospheric neutrinos [3,4] and derivation of oscillation parameters. Here we mention some features of the calculational scheme and use it to illustrate the basic features of a three-dimensional calculation.

1. Introduction

There are now several three-dimensional calculations of the atmospheric neutrino flux [5,6,7], which display the characteristic geometrical features described in [8] and reviewed in [9]. In developing this new calculation we have used the same three-dimensional version of the interaction model TARGET2.1 [10] that has previously been used in the context of one-dimensional cascade calculations for comparison with several other calculations of the flux of atmospheric neutrinos (see e.g. [9]). In this way we can compare the three-dimensional and one-dimensional calculations using the identical treatment of hadronic interactions. For both 3D and 1D we also use the same primary spectrum and composition; namely, the solar minimum flux from [2]. Further development of the TARGET interaction model itself is presented elsewhere in this conference [11].

For the three-dimensional calculation cascades are generated at discrete primary energies, equally spaced in $\log(\text{energy per nucleon})$, ten energies per decade. Cascades are generated separately for free protons, bound protons and bound neutrons within the superposition approximation. Nucleons are injected randomly and uniformly on the surface of a sphere of radius $R_{\oplus} + 80$ km, with a zenith angle distribution proportional to $\cos \theta_p$ and isotropically in local azimuth. Every neutrino that intersects the surface of the Earth within 500 km of the detector location is provisionally recorded with a weight proportional to the primary

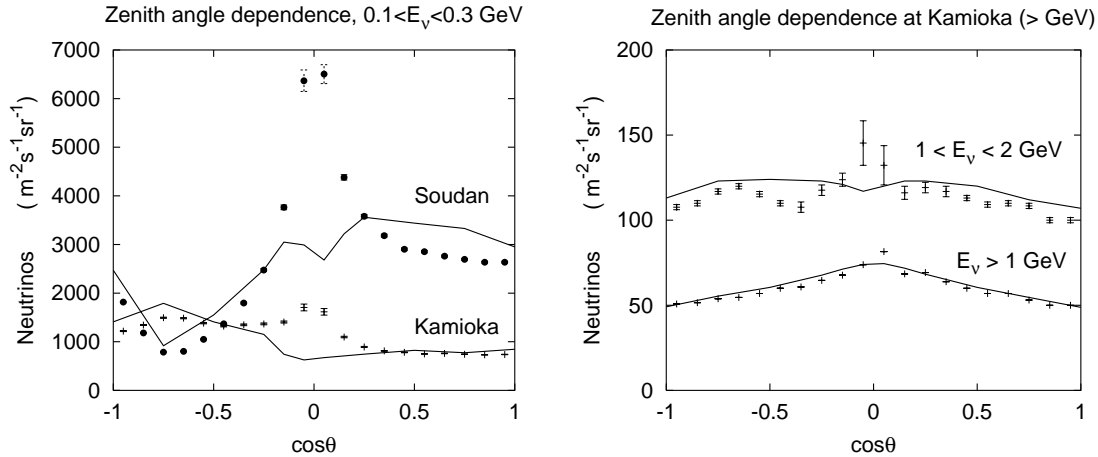


Fig. 1. Zenith-angle distributions at low energy comparing two locations (left panel) and for GeV neutrinos at Kamioka (right panel). points: 3D; lines: 1D.

spectrum of its parent nucleon multiplied by $1/\cos\theta_\nu$. Here θ_p is the local zenith angle of the primary nucleon at the injection sphere and θ_ν the local zenith angle of the neutrino when it intersects the sphere at the level of the detector. The last factor in the weight accounts for the projection of the flat detector, and its treatment requires special care near the horizon, as discussed elsewhere at this conference [12]. The parent nucleon of each provisionally accepted neutrino is backtracked from its point of injection, and the neutrino is accepted if its parent is on an allowed trajectory. (Bound nucleons are followed as particles of charge $-e/2$.) The fact that each neutrino carries the spectral weight of the primary that produced it means that a single set of cascade calculations can be re-weighted to reproduce any primary spectrum and composition without a time-consuming new calculation.

A three-dimensional Monte Carlo simulation of atmospheric neutrino fluxes has to face the problem that the actual size of the detector covers only a tiny fraction of the Earth's surface. In order to achieve reasonable statistics we use an acceptance radius of 500 km which is more than four orders of magnitude larger than the actual detector. Biases resulting from the use of a large effective detector area cancel provided that variations are linear across the acceptance area centered on the location of the actual detector. To insure that this requirement is satisfied we have repeated the calculations at intervals between 500 km and 2000 km along lines of latitude and longitude in each direction from the locations of Super-K [3], and SNO [7]. The largest changes are in the North-South direction because of the changing geomagnetic latitude, and they become significantly non-linear on scales of 1000 km and larger.

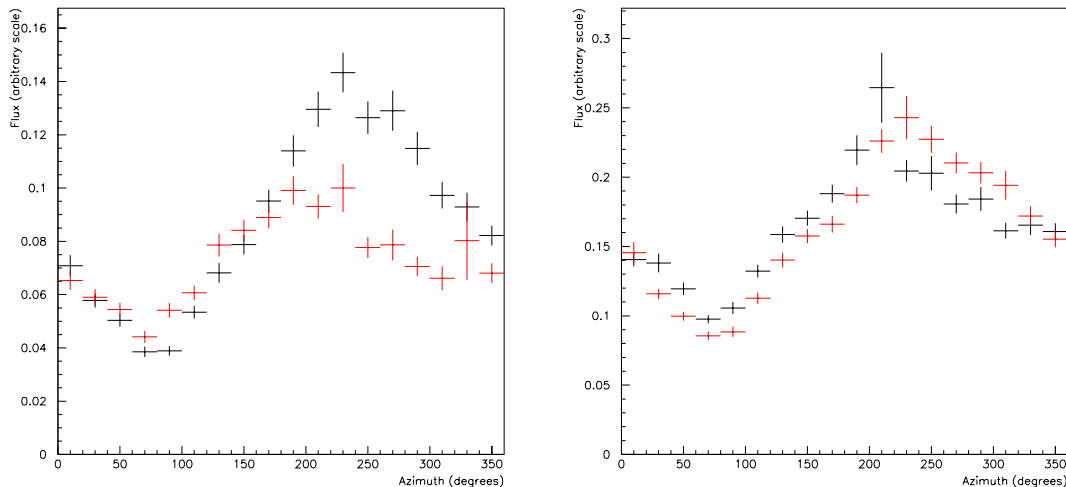


Fig. 2. Azimuthal distributions of neutrinos with $E > 0.5$ GeV and $-0.5 \leq \cos \theta \leq 0.5$. Left panel: ν_e (black) and $\bar{\nu}_e$ (grey/red); Right panel: ν_μ (solid/black) and $\bar{\nu}_\mu$ (dotted/red).

2. Comparison of 1D and 3D calculations

We have made a full 3D calculation of neutrino fluxes up to 10 GeV, which we compare with results of the one-dimensional calculation described in Reference 10. The first figure compares the angular distributions in the one-dimensional (straight-ahead) approximation with those obtained in the full 3D calculation. The characteristic enhancement near the horizontal is larger for the high-geomagnetic-latitude site where the geomagnetic cutoff is lower. The 1D calculation in fact gives a slight dip near the horizontal because of the large cutoff just above the horizon from the East. In the 1D calculation, the parents of all neutrinos from this direction are subject to the very high cutoff. In the 3D calculation, on the other hand, neutrinos near the horizon can arrive from primaries from a variety of directions. In fact the geometry favors production by relatively nearby interactions of primaries with smaller zenith angles. The small effect of this shortening of pathlengths for neutrinos near the horizon on inferred oscillation parameters remains to be investigated quantitatively.

The second figure shows the azimuthal distribution of neutrinos and antineutrinos at Super-K. More neutrinos arrive from the West (270°) than from the East (90°), but the asymmetry is greater for ν_e than for $\bar{\nu}_e$ and greater for $\bar{\nu}_\mu$ than for ν_μ . As pointed out in [13], such an effect can be traced to the fact that bending of positive muons enhances the East-West effect on the positive primaries whereas bending of negative muons is in the opposite sense. Thus the asymmetry is enhanced for progeny of μ^+ (i.e. ν_e and $\sim \frac{1}{2}$ of the $\bar{\nu}_\mu$) and decreased for $\bar{\nu}_e$

and $\sim \frac{1}{2}$ of the ν_μ . An interesting feature is that the azimuthal distribution is not symmetric about 180° , but is peaked around 220° rather than 270° , presumably a consequence of the geomagnetic field as seen from Super-K. (See e.g. Figure 10 of [9]).

ACKNOWLEDGEMENT. This research is supported in part by a grant DE-FG0291ER from the US Dept. of Energy, by UK PPARC and by INFN. One of us (TKG) is grateful for support from the Leverhulme Trust of the UK during his stay at Oxford.

1. Barr G. et al. 1989, Phys. Rev. D39, 3532
2. Agrawal V. et al. 1996, Phys. Rev. D53, 1314
3. Fukuda Y. et al. 1998, Phys. Rev. Lett. 81, 1562
4. Allison W.W.M. et al. 1999, Phys. Lett. B449, 137
5. Battistoni G. et al. 2000, Astropart. Phys. 12, 315
6. Honda M. et al. 2001, Phys. Rev. D64, 053011
7. Tserkovnyak Y. et al. 2003, Astropart. Phys. 18, 449
8. Lipari P. 2000, Astropart. Phys. 14, 153
9. Gaisser T.K. & Honda M. 2002, Annu. Rev. Nucl. Part. Sci. 52, 153
10. Engel R. et al. 2001, Proc. 27th ICRC (Hamburg) 1381
11. Engel R. et al. 2003 (this Conference)
12. Barr G. et al. 2003 (this Conference)
13. Lipari P. 2000, Astropart. Phys. 14, 171